Genomic differentiation is initiated without physical linkage among targets of divergent selection in Fall armyworms

Kiwoong Nam[1*], Sandra Nhim[1], Stéphanie Robin[2,3], Anthony Bretaudeau[2,3], Nicolas Nègre[1], Emmanuelle d'Alençon[1]

[1]DGIMI, INRA, Univ. Montpellier, 34095, Montpellier, France
[2]INRA, UMR-IGEPP, BioInformatics Platform for Agroecosystems Arthropods, Campus Beaulieu, Rennes, 35042, France
[3]INRIA, IRISA, GenOuest Core Facility, Campus de Beaulieu, Rennes, 35042, France
* corresponding author (ki-woong.nam@inra.fr)

ABSTRACT

The process of speciation involves the differentiation of whole genome sequences. Gene flow between population impedes this process because recombination in hybrids homogenizes sequences. Accumulating empirical cases demonstrate that speciation indeed occurs in the presence of gene flow, and several speciation models have been proposed to explain the process of whole genome differentiation. Polymorphism patterns from a pair of very recently diverged taxa may provide insightful information to identify critical evolutionary forces enabling genomic differentiation. The Fall armyworm, *Spodoptera frugiperda* is observed as two sympatric strains, corn strain, and rice strain, named from their preferred host plants, throughout the entire range of habitats. The difference in host-plant ranges suggests a possibility of ecological divergent selection. In this study, we analyzed whole genome sequences from these two strains from Mississippi based on population genetics approaches and *de novo* genome assembling to study initial steps toward genomic differentiation. The genomic Fst is low (0.017), while 91.3% of 10kb windows have Fst greater than 0, suggesting genome-wide differentiation with a low extent. Principal component analysis and phylogenetic analysis show that corn strains were derived from ancestral rice strains and these two strains experienced population expansion with a greater extent in corn strains. We identified only three strain-specific chromosomal rearrangements, and the role these rearrangements in genomic differentiation is not supported. We identified 423 and 433 outliers of genetic differentiation between strains from the mappings against the reference genomes of corn and rice strains, respectively. Among them, four and nine outliers have a higher level of absolute sequence divergence (d_{XY}) than genomic average from these two mappings, and these outliers contain genes related to female fecundity. The rest of outliers have a reduced level of genetic diversity suggesting signatures of selective sweeps. In these outliers, corn strains have diverged genotypes from rice strains, and this divergence is observed only from the flanking sites in which the distance from the nearest outliers is less than 1kb, implying that physical linkage among outliers is unimportant for genomic differentiation. Gene density is negatively correlated with nucleotide diversity, but not with Fst. This result suggests that, while the level of local genetic diversity is affected by the strength of selection, selection is not a primary source of local variation in genomic differentiation, and genomic reduction in migration rate is the most likely reason for genomic differentiation. From these results, we proposed that in *S.frugiperda* divergence female fecundity traits caused the initiation of genetic difference and that following divergent selection targeting many loci results in the reduction in genomic migration rate, which creates genome-wide genetic differentiation. This explanation is in line with the genome hitchhiking model.

INTRODUCTION

Gene flow impedes the process of speciation because recombination in hybrids homogenizes sequences between populations[1]. An exceptional condition is, therefore, necessary to overcome the homogenizing effect of gene flow (reviewed in [2]). As speciation processes inherently involve genomic differentiation by reproductive barriers, generated through collective or sequential actions of evolutionary forces[3], how the homogenizing effect of recombination is overcome throughout whole genomes is a key issue to understand the speciation process[4]. Accumulating empirical reports show that speciation indeed occurs in the presence of gene flow[5], implying that the homogenizing effect of recombination can be effectively overcome.

Divergent selection is one of the main players occurring during the process of speciation. If selection is sufficiently strong (i.e, $s > m$[6] or $s > r$[7], where s, m, and r are selection coefficient, migration rate, and recombination rate, respectively), the effect of selection dominates that of gene flow and recombination, thus genomic differentiation may not be hampered by gene flow. If selection is weak ($s < m$ and $s < r$), other conditions are necessary for genomic differentiation. Physical linkage among the targets might be responsible for genomic differentiation, as selective sweeps[8] increase in the level of genetic differentiation at sites physically linked to the targets of divergent selection. For example, if divergent selection targets a large number of loci, then the average physical distance from a neutral locus to the targets decreases, thus whole genome sequences can be differentiated by the concerted actions of divergent selection[9]. In another speciation model, termed divergence hitchhiking, if a locus is targeted by strong divergent selection, then the effective rate of migration is reduced in this region, and following events of divergent selection targeting sequences within this region may generate a long stretch of differentiated DNA (up to several Mb)[10,11]. Population-specific chromosomal rearrangements can also contribute to the process of speciation because recombination is inhibited in hybrids[12–15] and physical linkage between targets of divergent selection and the loci with a chromosomal rearrangement may create long genomic regions with differentiation[16]. Whole genome sequences may be also differentiated without physical linkage among targets of selection. According to the genome hitchhiking model, if divergent selection targets many loci, then genome-wide migration rate is effectively reduced, and whole genome sequences can be differentiated[17,18].

If the number of targeted loci is sufficiently high, genomic differentiation may occur rapidly. The loci targeted by population-specific divergent selection may have correlated allele frequencies, and corresponding linkage disequilibrium among targets will be then generated[6,19,20]. Theoretical studies[6,19] show that if the number of targets is higher than a certain threshold, targeted loci have a synergistic effect in increasing linkage disequilibrium among targets, thus genomic differentiation is consequently accelerated. This non-linear dynamics of genomic differentiation according to the number of occurred selection events were termed genome-wide congealing[21]. It should be noted that any diversifying factors, including divergent selection, background selection, and assortative mating[22], may contribute to genome-wide congealing. Thus, the critical question of how genomic differentiation occurs in the presence of gene flow is the condition for the transition to the phase of genome-wide congealing. For example, divergence hitchhiking may provide a condition for post-genome-wide congealing phase[4]. Alternatively, genome-wide reduction in migration rate (genome hitchhiking) or chromosomal rearrangement may contribute to this condition as well.

Divergence hitchhiking model has been supported by pea aphids[10], stickleback[23], and poplar[24]. However, as Feder and Nosil demonstrated[18], long differentiated sequences can be observed only from a specific condition, when effective population size (Ne) and migration rate are low (Ne = 1,000, m = 0.001), and selection is very strong (s = 0.5). Isolation by adaptation, a positive correlation between a genetic difference and adaptive divergence[25,26], has been presented as a

support for genome hitchhiking, which indeed causes isolation by adaptation[4]. However, it is still unclear whether genome hitchhiking initiates or reinforces genetic differentiation in cases of isolation by adaptation.

The Fall armyworm, *Spodoptera frugiperda*, (Lepidoptera, Noctuidae) is a pest species observed as two sympatric strains, corn strain (sfC hereafter) and rice strain (sfR) named from their preferred host-plants, throughout North and South American continents[27]. Based on maker-genotyping, these two strains appear to have different DNA sequences[27,28]. In a wide geographical range in North America, 16% of individuals were reported to be hybrids[29], suggesting frequent gene flow between strains. In our previous study, we observed that these two strains have a weak but significant genomic differentiation (Fst = 0.019, $p < 0.005$), and that the differentiated loci were distributed across the genome[30]. Low level of genomic differentiation and widespread occurrence of hybrids make these two strains an ideal system to explore critical evolutionary forces for genomic differentiation in the presence of gene flow. Whole genome differentiation between sfC and sfR might involve both premating reproductive isolation through assortative mating[31–33], or postmating reproductive isolation by ecological divergent selection, or by reduced hybrid fertility[34] .

In this study, we aim at identifying evolutionary forces that are responsible for genomic differentiation between sfC and sfR at the very initial stage of the speciation process. Using resequencing data generated in our previous study[30], we test the role of several evolutionary events in genomic differentiation, including chromosomal rearrangements, physical linkages among targeted loci, and genomic reduction in migration rate. The results presented here allow us to infer the evolutionary history explaining the genomic differentiation between strains in *S.frugiperda*.

RESULTS

In order to accurately detect signatures of genome divergence, it is important to have a contiguous reference genome assembly. The reference genome assemblies for sfC and sfR generated from our previous study contain 41,577 and 29,127 scaffolds, respectively[30] (Table 1). To improve the reference genome sequences we performed *de novo* genome assembly from Pac-bio reads (27.5X and 33.1X coverages for sfC and sfR, respectively). Errors in these reads were corrected by Illumina assemblies, which were generated from the reads used in our previous study[30]. The Pac-bio reads were assembled using SmartDenovo[35], and scaffolding was performed using Illumina paired-ends and mate-pairs used in our previous study. The resulting assemblies are now closer to the expected genome sizes, 396±3Mb, estimated by flow cytometry[30] (Table 1). Moreover, the contiguity is also significantly improved, as N50 is 900kb and 1,129kb for corn and rice reference genome sequences, respectively. The numbers of sequences are 1,000 and 1,054 for sfC and sfR, respectively. BUSCO analysis[36] shows that the correctness is also increased, especially for the sfC (Supplementary Table 1). The numbers of identified protein-coding genes are 21,839 and 22,026 for sfC and sfR, respectively. BUSCO analysis shows that gene annotation is also improved, especially for sfC (supplementary Table 2).

Resequencing data from nine female individuals from each of corn and rice strains collected in the wild[30] were mapped against these two nuclear reference genome assemblies using bowtie2[37] with very exhaustive search parameters (see methods). As one individual from rice strain has a particularly low mapping rate and an average read depth (denoted as R1, Gouin et al[30]) (Supplementary Figure 1), we excluded this individual from the following analysis. Variants were called using samtools mpileup[38], and we performed stringent filtering by discarding all sites unless Phred variant calling score is higher than 40 *and* genotypes are determined from every single individual. The numbers of variants are 48,981,416 from 207,415,852 bp and 49,832,320 from 205,381,292 bp from the mapping against sfC and sfR reference genomes, respectively. As analyses

from the resequencing data might be affected by ascertainment bias, we performed all analyses based on these two reference genomes. We present the results only from the sfC reference genomes in the main text unless mentioned specifically. We show the results from the sfR reference genome in the supplementary information (Supplementary Figure 14-21).

The genome-wide Fst calculated between sfC and sfR is 0.017, which is comparable to our previous study (0.019)[30]. As this low level of differentiation could be caused by chance, we calculated Fst from randomized groupings with 500 replications. We observed that no randomized grouping has higher Fst than the grouping according to strains (equivalent to $p < 0.002$), thus we concluded that the genomic sequences are significantly differentiated between strains, as we did in our previous study[30]. This genomic differentiation can be either caused by a few loci with a very high level of differentiation or by many loci with a low level of differentiation. To test these two possibilities, we calculated Fst in 10 kb window. Among total windows, 91.3% of these windows have Fst greater than 0 (Figure 1), supporting the latter explanation. The low level of genetic differentiation implies that these two strains do not experience genome-wide congealing yet.

Genetic relationships among individuals were inferred using principal component analysis (PCA). The result shows that sfR has a higher genetic variability among individuals than sfC, and we hypothesized that sfC was derived from ancestral sfR (Figure 2a). To test this hypothesis, we reconstructed a phylogenetic tree using assembly-free approach[39] with *S.litura*[40] as an outgroup. The resulting tree shows that sfC individuals constitute a monophyletic group, implying that the sfC was indeed derived from ancestral sfR (Figure 2b). The pattern of the phylogenetic tree is subtly different from that of PCA. The phylogenetic tree shows that sfC has monophyly, implying that the sfC individuals were derived from a single individual. However, the result from PCA does not support the single origin of sfC. This discrepancy is perhaps caused by an incomplete lineage sorting in the ancestry of sfC or by frequent gene flow between sfC and sfR. However, we cannot exclude a possibility that statistical artifacts, such as long-branch attractions[41]. The genetic relationship among individuals was also analyzed from ancestry coefficient[42], and we observed that distinct origins of sfC and sfR are not supported (Supplementary Figure 2).

We tested the possibility of an extreme case where both sfC and sfR have monophyly, but all identified sfR individuals except R6 on Figure 2b are F1 hybrids between sfR females and sfC males. In this case, maternally-derived mitochondrial CO1 genes used to identify strains in this study[30] will have distinctly different sequences between R2-R9 and C1-C9, while paternally derived sequences will not show such a pattern between these two groups except R6. As all individuals analyzed in this study are females, the Z chromosomes were derived from males in the very previous generation. Thus, we tested significant genetic differentiation of Z chromosomes between sfC and sfR without R6. TPI gene is known to be linked to Z chromosomes in *S.frugiperda*[43], and we observed this gene from Contig269 by blasting. This contig is 3,688,019bp in length, and the number of variants is 201,075. The Fst calculated between sfC and sfR without R6 is 0.061, which is higher than the genomic average (0.017). We calculated Fst from randomized groupings with 500 replicates, and only four replicates have Fst higher than 0.061, corresponding p-value equal to 0.008. This result demonstrates a significant genetic differentiation of paternally derived Z chromosomes between strains identified by mitochondrial sequence, and we exclude the possibility of the extreme case with F1 hybrids.

We inferred changes in *Ne* from two statistics, π and Watterson's θ. Watterson's θ represent more recent levels of genetic diversity than π. The calculated π is 0.043 and 0.044 for sfC and sfR, respectively. The π is not significantly different between sfC and sfR ($p=0.27$, permutation test with 100 randomizations). The calculated Watterson's θ is 0.064 and 0.061 for sfC and sfR,

respectively, and sfC has higher Watterson's θ than sfR ($p < 0.01$). This result indicates that both sfC and sfR experienced population expansion with a greater extent in sfC, possibly due to higher fitness in sfC.

Chromosomal rearrangements specific to a single population can cause a genetic differentiation because recombination is inhibited in hybrids[12,13,15]. Thus, we estimated the role of chromosomal rearrangements in genomic differentiation by identifying the propensity of strain-specific chromosomal rearrangements. Using BreakDancer[44] we identified 1,254 loci with chromosomal inversions, with 1,060bp in median sequence length. We considered that a chromosomal rearrangement is strain-specific if the difference in allele frequency is higher than an arbitrarily chosen criterion, 0.75. Fst calculated from these inversions are lower than zero (-0.063 and -0.064), meaning that the contribution of chromosomal inversion to genetic differentiation is not supported. The number of inter-scaffold rearrangement is 1,724, and only one of them has a difference in allele frequency higher than 0.75. Fst calculated from 10kb flanking sequences of the breaking points is lower than zero (-0.115 and -0.0783 at each side). Thus, we excluded the possibility that chromosomal rearrangement is a principal cause of genomic differentiation.

Then, we test the possibility that selection is responsible for genomic differentiation from outliers of genetic differentiation. We used correlated haplotype score[45] to estimate the level of genetic differentiation between strains. If each of minimum 100 consecutive SNPs in minimum 1kb has a significantly greater haplotype score than the rest of the genome ($p < 0.001$), we defined this locus as an outlier. As the mapping rate of reads against highly differentiated sequences is necessarily low, the identification of outliers can be severely affected by the usage of reference genome sequences. Therefore, here we present the results from both corn and rice reference genome sequences (refC and refR). In total, 433 outliers at 170 scaffolds and 423 outliers at 148 scaffolds were identified from the mappings against refC and refR, respectively. The average length of these outliers is 4,023bp and 4,095bp for refC and refR, respectively. The longest outlier is 27,365bp and 33,110bp in length for refC and refR, respectively. These outliers occupy only small fractions of the scaffolds (1.56% and 1.82% for refC and refR, respectively), suggesting that extremely strong selective sweeps are not supported. Thus, it is unlikely that very strong selection targeting these regions causes whole genome differentiation.

We test the possibility of the divergence hitchhiking[10], a hypothesis that a strong selection creates DNA sequences with reduced local migration rate, and following selection events within this sequence generates a long stretch of DNA sequence with an elevated level of genetic differentiation. According to this speciation model, lowly differentiated sequences between highly differentiated sequences are generated by ancestral polymorphisms, rather than gene flow[10]. Thus, these lowly differentiated sequences between highly differentiated sequences will show clustered ancestry maps according to the extant strains, whereas the rest of lowly differentiated sequences in the genome will not show such a clustering. From the scaffolds with the outliers, we identified lowly differentiated sequences (hapflk score < 1, Supplementary Figure 3 to see the histogram of all positions at these scaffolds), 154,163bp and 273,797bp in total size from refC and refR, respectively. Then, sNMF software was used to infer ancestry coefficients[42]. Figure 3 shows that sfC and sfR have different ancestry at outliers, while the lowly differentiated sequences within the scaffolds with outliers do not show any apparent clustering according to extant strains. Thus, divergence hitchhiking is not supported by our data.

If a genetic locus is resistant against gene flow from the beginning of genetic differentiation, this sequences is expected to show a higher level of absolute genetic divergence, which can be estimated from d_{XY} statistics[46]. We observed that four out of the 433 outliers from refC and nine out of the 423

outliers from refR have higher d_{XY} than genomic average (FDR corrected $p < 0.05$) (Supplementary Figure 4, 5). We denote these outliers as genomic islands of divergence in this paper. These genomic islands of divergence contain three and four protein-coding genes from refC and refR, respectively. These genes include NPRL2 and Glutamine synthetase 2. NPRL2 is a down-regulator of TORC1 activity, and this down-regulation is essential in maintaining female fecundity during oogenesis in response to amino-acid starvation in Drosophila[47]. Glutamine synthetase 2 is important in activating TOR pathway, which is the main regulator of cell growth in response to environmental changes to maintain fecundity in plant hoppers[48]. This result raises the possibility that disruptive selection on female fecundity is responsible for initiating genetic differentiation between strains. The function of the other five genes is unclear, thus other traits might be important in initiating genomic differentiation as well.

If genetic differentiation is initiated by selection on female fecundity, mitochondrial genomes will show a higher level of absolute level of sequence divergence than nuclear genome because mitochondrial genomes are transmitted only through the maternal lineage. We performed mapping all reads against mitochondrial genomes (KM362176) and identified 371 variants from 15,230bp. The result from PCA shows that, contrary to the nuclear pattern, sfC and sfR individuals fall into two distinct groups (Figure 4a). Ancestry coefficient analysis shows that each of two strains has a distinct ancestry (Figure 4b) (see Supplementary Figure 6 to find a correlation between K and cross entropy). To generate a mitochondrial phylogenetic tree, we extracted sequences of *S.frugiperda* from mitochondrial Variant Call Format file, and we created a multiple sequence alignment together with the mitochondrial genome sequence of *S.litura* (KF701043). Then, a phylogenetic tree was reconstructed using the minimum evolution approach[49]. The tree shows that sfC and sfR are a sister group of each other(Figure 4c). This mitochondrial pattern is also observed from other studies in *S.frugiperda*[28,30,50]. We excluded a possibility that strong linked selection on mitochondrial genomes alone causes the different phylogenetic pattern between nuclear and mitochondrial genomes because in this case the topology is expected to be unchanged while only relative lengths of ancestral branches to tips are different between nuclear and mitochondrial trees (Supplementary Figure 7). Instead, this pattern can be explained by an ancient divergence of mitochondrial genomes, which is followed by a gradual genetic differentiation of nuclear genomes.

A molecular clock study shows that the mitochondrial genomes diverged between sfC and sfR two million years ago[28], which corresponding 2×10^7 generations according to the observation from our insectarium (10 generations per year). Assuming that the *Ne* is 4×10^6 for both strains, the number of generations during this mitochondrial divergence time is five times of *Ne*. We performed a simple forward simulation[51] with a wide range of migration rate to test this divergence time can explain the level of observed genetic differentiation (Fst = 0.017). No simulation generates Fst equal or lower than 0.017 (Supplementary Figure 8), supporting that mitochondrial genomes diverged more anciently than nuclear genomes.

We investigated the role of the rest of outliers, denoted by genomic islands of differentiation in this paper. Genomic islands of differentiation have much lower π than the genomic average in both strains (Supplementary Figure 9), and sfC has a lower π than sfR ($p = 0.0007$; Wilcoxon rank sum test), suggesting that the genomic islands of differentiation were targeted by linked selection, as a form of selective sweeps[8] or background selection[52], with a greater extent in sfC. d_{XY} calculated from genomic islands of differentiation is on average lower than the genomic average (Supplementary Figure 10), suggesting that these sequences were targeted by linked selection targeted after the split between sfC and sfR. PCA from genomic islands of divergence and genomic islands of differentiation shows that these two types of genomic islands have a clear grouping according to strains (Figure 5), which was observed from mitochondrial genomes (Figure 4a) but

not from nuclear genomes (Figure 2a). Interestingly, the sequences of genomic islands of divergence have comparable genetic variability between sfC and sfR, whereas sfC has a lower genetic variability in the sequence of genomic islands of differentiation than sfR. From these results, we concluded that the sfC diverged from sfR by linked selection.

We investigated the role of physical linkage by performing PCA with varying distances to the nearest genomic island of differentiation. When the distance is less than 1kb, genetic variations of sfC individuals are included within the range of genetic variation of sfR individuals (PC1 of the leftmost panel at Figure 6), while divergence of sfC from sfR is also supported (PC2 of the leftmost panel at Figure 6). If the distance is higher than 1kb, the divergence of sfC from sfR is not observed (Figure 6), suggesting that the effect of physical linkage to genomic islands of differentiation disappears rapidly as the distance increases. The short linkage disequilibrium in a species with large *Ne* is expected from a theoretical analysis[18], and reported from empirical cases[53,54]. These results show that physical linkages among targets of linked selection are not the primary cause of genomic differentiation.

Then, we tested a possibility of genome hitchhiking[17,18], a hypothesis stating that genomic differentiation is caused by a genome-wide reduction in migration rate due to many loci under selection. If the strength of selection determines the level of genetic differentiation, a positive correlation between Fst and the strength of selection is expected. Alternatively, if a genomic reduction in migration rates dominates the effect of selection, this correlation is not expected. We assume that the exon density is a proxy for the strength of selection. Exon densities calculated in 100kb window are negatively correlated with π (Spearman's $\rho = -0.211$, $p < 2.2 \times 10^{-16}$) (Figure 7), showing that the local genetic diversity pattern is affected by selection. Fst, however, is not significantly correlated with exon density ($\rho = 0.021$, $p = 0.2032$) (Figure 7). This result supports the hypothesis that a genomic reduction in migration rate dominates the variation of genetic differentiation.

In principle, both selective sweeps and background selection may target these genomic islands of differentiation as linked selection. Background selection may cause genetic differentiation between populations only if these two populations are *a priori* differentiated by a geographical separation or a tight physical linkage to a target of selective sweeps. As sfC and sfR are sympatrically observed and the physical linkage among genomic islands of differentiation is not supported as shown above, we assume that selective sweeps are mainly responsible for the genomic islands of differentiation and inferred traits under adaptive evolution from the function of genes within genomic islands of differentiation. These islands contain 275 and 295 protein-coding genes from refC and refR, respectively (the full list can be found from Supplementary Table 3-4). These protein-coding sequences include a wide range of genes important for the interaction with host-plants, such as P450, chemosensory genes, esterase, immunity gene, and oxidative stress genes[30] (Table 2), suggesting that ecological divergent selection is important for genomic differentiation. Interestingly, cyc gene, which plays a key role in circadian clock[55], is also included in the list of the potentially adaptively evolved genes. Thus, divergence selection on cyc may be responsible for pre-mating reproductive isolation due to allochronic mating time[31,32].

A QTL study shows that genetic variations in vrille gene can explain differentiated allochronic mating behavior in *S.frugipera*[31]. This gene is not found in the outliers. Fst calculated from a 10kb window containing this gene is 0.017 and 0.016 for refC and refR, respectively, which is similar to genomic average (0.017). Thus, it appears that this gene does not have a direct contribution to genomic differentiation.

DISCUSSION

In this study, we showed that genetic differentiation between strains in *S.frugiperda* is initiated by the divergence of genes associated with female fecundity from the gene list in the genomic islands of divergence (Figure 8 to see a possible evolutionary scenario of genetic differentiation between sfC and sfR). Afterward, divergent selection targeting many loci appears to reduce the genome-wide migration between strains, which have low but significant genome-wide genetic differentiation, in line with the genome hitchhiking model[17,18]. The physical linkage among targets of linked selection appears to be unimportant for genomic differentiation in *S.frugiperda*. We observed that genomic islands of differentiation contain genes associated with interaction with host-plants, thus the adaptive evolution of this ecological trait appears to promote genomic differentiation between strains. A circadian gene (cyc) is also found from a genomic island of differentiation, and it is unclear whether this gene is associated with the assortative mating due to allochronic mating patterns in *S.frugiperda*. If this is true, both divergent selection and assortative mating generate genomic differentiation by a genomic reduction in migration rate between strains, since assortative mating generates the same footprints on DNA sequences as divergent selection.

The heterozygosity of these strains is unprecedented high, as the calculated π is 0.043-0.044. In two other Noctuid pests, *S.litura* and *Helicoverpa armigera*, π calculated from multiple populations across their distribution area ranges from 0.0019 to 0.016[40], and from 0.008 to 0.01[56], respectively. *Heliconius melpomene*, a butterfly species, has π between 0.021 and 0.029[57]. To explain the extremely high level of heterozygosity in *S.frigiperda*, we first checked the possibility that a considerable proportion of identified variants is false positives. We performed additional filterings, on the top of applied ones, by including additional 12 criteria. These additional filterings discarded only 34 out of 48,981,416 and 17 out of 49,832,320 variants from the mapping against refC and refR, respectively. Thus, we exclude the possibility that false positives caused the high level of heterozygosity. We inferred past demographic history using pairwise sequentially Markovian coalescent[58] based on assumptions that generation time is the same with lab strains at our insectarium (10 generation/yr) and mutation rate is the same with *H.melpomene* (2.9×10^{-9}/site/generation)[59]. Extremely rapid population expansions were inferred from both two strains (*Ne* was increased from 9.6×10^5 to 1.2×10^7) between 10 mya and 100 mya (Supplementary Figure 11). A possible explanation of this rapid expansion is the merge of genetically diverged ancestral populations by hybridization. In this scenario (Figure 8), two populations were separated by geographical barriers and genetically differentiated. At some moment, the geographical barriers were removed, and these populations started to be merged by hybridization. As the merged population maintains a large proportion of variants, this population has a high level of heterozygosity. This population is extant sfR. Afterward, a group of sfR started to diverge by ecological divergent selection, and assortative mating and this group became the extant sfC.

The pattern of genomic differentiation can be different among geographic populations. For example, pairs of different geographical populations may have different levels of genomic differentiation (Fst). The genomic islands of differentiation can be also different if a proportion of divergent selection is specific to a single geographical population, thus it is worthwhile to test if the same loci are identified as genomic islands of divergence across diverse geographic populations. If levels of genomic differentiation vary among different geographical populations in *S.frugiperda*, it might be possible to find a pair of strains that enter to a phase of genome-wide congealing. Attempts to find the process towards complete genomic differentiation, often called ‘speciation continuum’, are typically based on closely related multiple species[60,61]. However, different species may have experienced very different evolutionary histories. Thus, studying a single species with

varying levels of genetic differentiation might shed light on the exact process of genomic differentiation.

Several genetic markers have been proposed to identify strains, including mitochondrial CO1[62], sex chromosome FR elements [63], and Z-linked TPI[43]. We found that FR elements are a reliable marker to identify strains (Supplementary Figure 12). TPI is included in the gene list within the genomic island of differentiation, and d_{XY} from TPI (0.0345) is slightly lower than genomic average (mean is 0.0384 with 0.0383-0.0386 of 95% confidence interval). Thus, the genetic differentiation of TPI appears to occur after the initiation of genetic differentiation between sfC and sfR. The concordance of identified strains between mitochondrial CO1 and TPI can be as low as 74% (Table 5 at [43]), and this imperfect concordance might be due to the different divergence time. Thus, we propose to use mitochondrial markers to identify strains for unambiguous strain identification.

The process of speciation proposed in this study can be further tested based on insect rearing or lab experiments (such as CRISPR/CAS9). For example, we proposed in this study that female fecundity could be a key trait that initiated genetic differentiation between strains because genes associated with this trait appears to have a resistance against gene flow. The reason for this resistance can be a reduction in hybrid fitness, and we can test this possibility by insect-rearing. We also raise a possibility in this paper that cyc gene might be associated with allochronic mating behavior, and we can test this possibility using CRISPR/CAS9 experiment as well. These future studies will shed light on the relationship between genotypes and phenotypes that plays critical roles in the process of speciation.

METHOD

We extracted high molecular weight DNA using MagAttract© HMW kit (Qiagen) from one pupa of sfC and two pupae of sfR with a modification of the original protocol to increase the yield. The quality of extraction was assessed by checking DNA length (> 50kb) on 0.7% agarose gel electrophoresis, as well as pulsed-field electrophoresis using the Rotaphor (Biometra) and gel containing 0.75% agarose in 1X Loening buffer, run for 21 hours at 10°C with an angle range from 120 to 110° and a voltage range from 130 to 90V. DNA concentration was estimated by fluorimetry using the QuantiFluor Kit (Promega), 9.6 µg and 8.7 µg of DNA from sfC and sfR, respectively, which was used to prepare libraries for sequencing. Single-Molecule-Real-Time sequencing (12 SMRT cells per strain, equivalent to expected genome coverage of 20x) was performed using a PacBio RSII (Pacific Biosciences) with P6-C4 chemistry at the genomic platform Get-PlaGe, Toulouse, France (https://get.genotoul.fr/). The total throughput is 11,017,798,575bp in 1,513,346 reads and 13,259,782,164bp in 1,692,240 reads for sfC and sfR, respectively. The average read lengths are 7,280bp and 7,836bp for sfC and sfR, respectively.

We generated assemblies from Illumina paired-end sequences[30] (166X and 308 X coverage for sfC and sfR, respectively) using platanus[64]. Then, errors in PacBio were corrected using Ectools[65], and uncorrected reads were discarded. The remaining reads are 8,918,141,742bp and 11,005,855,683bp for sfC and sfR, respectively. The error-corrected reads were used to assemble genome sequences using SMARTdenovo[35]. The paired-end Illumina reads were mapped against the genome assemblies using bowtie2[37], and corresponding bam files were generated. We improved the genome assemblies with these bam files using pilon[66].

For the genome assemblies of sfC, both Illumina paired-end and mate-pair reads were mapped the genome assemblies using bwa[67], and scaffolding was performed using BESST[68]. Since only paired-end libraries were generated in our previous study[30], we used only paired-end sequences to perform scaffolding for sfR. The gaps were filled using PB-Jelly[69]. The correctness of assemblies was assessed using insect BUSCO (insecta_odb9)[36].

Then, protein-coding genes were annotated from the genome sequences using MAKER[70]. First, repetitive elements were masked using RepeatMasker[71]. Second, *ab initio* gene prediction was performed with protein-coding sequences from two strains in *S.frugiperda*[30] and *Helicoverpa armigera* (Harm_1.0, NCBI ID: GCF_002156995), as well as insect protein sequences from *Drosophila melanogaster* (BDGP6) and three Lepidoptera species, *Bombyx mori* (ASM15162v1), *Melitaea cinxia* (MelCinx1.0), and *Danaus plexippus* (Dpv3) in ensemble metazoa. For transcriptome sequences, we used reference transcriptome for sfC[72] and locally assembled transcriptome from RNA-Seq data from 11 samples using Trinity[73] for sfR. Third, two gene predictors, SNAP[74] and Augustus[75], were trained and gene annotations were improved. Multiple trainings of the gene predictors do not decrease Annotation Edit Distance Score, thus we used the gene annotation with only one training. Fourth, we discarded all gene prediction if eAED score is greater than 0.5.

Paired-end Illumina resequencing data from nine individuals from each of corn and rice strains in *S.frugiperda* is used to identify variants. Low-quality nucleotides (Phred score < 20) and adapter sequences in the reads were removed using AdapterRemoval[76]. Then, reads were mapped against reference genomes using bowtie2, with very exhaustive local search parameters (-D 25 -R 5 -N 0 -L 20 -i S,1,0.50), which is more exhaustive search than the –very-sensitive parameter preset. Potential PCR or optical duplicates were removed using Picard tool[77]. Variants were called using samtools mpileup[38] only from the mappings with Phred score higher than 30. Then, we discarded all called positions unless a genotype is identified from all individuals and variant calling score is greater than 40. We also discarded variants if the read depth is higher than 3,200 or lower than 20.

We used vcf tools to calculate population genetics statistics, such as π and Fst[78]. Watterson's θ and d_{XY} were calculated using house-perl scripts. To estimate the genetic relationship among individuals, we first converted VCF files to plink format using vcftools, then PCA was performed using flashpca[79]. For ancestry coefficient analysis, we used sNMF[42] with K values ranging from 2 to 10, and we chose the K value that generated the lowest cross entropy.

Phylogenetic tree of the nuclear genome was generated using AAF[39]. As an outgroup, we used simulated fastq files from the reference genomes of *S.litura* using genReads[80] with an error rate equal to 0.02. Reads were mapped against the mitochondrial genome (KM362176) using bowtie2[37] to generate the mitochondrial phylogenetic tree, and variants were called using samtools mpileup[38]. From the mitochondrial VCF file, a multiple sequence alignment was generated using house-perl script. Then, the whole mitochondrial genome from *S.litura* (KF701043) was added to this multiple sequence alignment, and a new alignment was generated using prank[81]. The phylogenetic tree was reconstructed from this new alignment using FastME[49] with 1,000 bootstrapping.

The outliers of genetic differentiation were identified from hapFLK scores calculated from hapflk software[45]. As the computation was not feasible with the whole genome sequences, we randomly divided sequences in the genome assemblies into eight groups. Fst distributions from these eight groups were highly similar between each other (Supplementary Figure 13). P-values showing the statistical significance of genetic differentiation were calculated from each position using scaling_chi2_hapflk.py in the same software package.

DATA AVAILABILITY

The reference genome and gene annotation are available from BioInformatics Platform for Agroecosystem Arthropods together with the genome browser (https://bipaa.genouest.org/is/). This data can be found at European Nucleotide Archive (https://www.ebi.ac.uk/ena) as well (project id:

PRJEB29161). Resequencing data is available from NCBI Sequence Read Archive. Corresponding project ID is PRJNA494340.

ACKNOWLEDGMENTS

This work was partially supported by a grant from SPE department at INRA (adaptivesv) for K.N., by a grant from the French National Research Agency (ANR-12-BSV7-0004-01; http://www.agence-nationale-recherche.fr/) for E.A., and by a grant from Institut Universitaire de France for N.N.

REFERENCE

1. Felsenstein, J. Skepticism towards Santa Rosalia, or why are there so few kinds of animals? *Evolution* **35**, 124–138 (1981).
2. Bolnick, D. I. & Fitzpatrick, B. M. Sympatric speciation: models and empirical evidence. *Annu. Rev. Ecol. Evol. Syst.* **38**, 459–487 (2007).
3. Wu, C.-I. The genic view of the process of speciation. *J. Evol. Biol.* **14**, 851–865 (2001).
4. Feder, J. L., Egan, S. P. & Nosil, P. The genomics of speciation-with-gene-flow. *Trends Genet.* **28**, 342–350 (2012).
5. Nosil, P. Speciation with gene flow could be common. *Mol. Ecol.* **17**, 2103–2106
6. Flaxman, S. M., Wacholder, A. C., Feder, J. L. & Nosil, P. Theoretical models of the influence of genomic architecture on the dynamics of speciation. *Mol. Ecol.* **23**, 4074–4088 (2014).
7. Barton, N. H. Gene flow past a cline. *Heredity* **43**, 333–339 (1979).
8. Smith, J. M. & Haigh, J. The hitch-hiking effect of a favourable gene. *Genet. Res.* **23**, 23–35 (1974).
9. Barton, N. & Bengtsson, B. O. The barrier to genetic exchange between hybridising populations. *Heredity* **57**, 357–376 (1986).
10. Via, S. Divergence hitchhiking and the spread of genomic isolation during ecological speciation-with-gene-flow. *Philos. Trans. R. Soc. Lond. B. Biol. Sci.* **367**, 451–460 (2012).
11. Via, S. & West, J. The genetic mosaic suggests a new role for hitchhiking in ecological speciation. *Mol. Ecol.* **17**, 4334–4345 (2008).
12. Rieseberg, L. H. Chromosomal rearrangements and speciation. *Trends Ecol. Evol.* **16**, 351–358 (2001).
13. Butlin, R. K. Recombination and speciation. *Mol. Ecol.* **14**, 2621–2635 (2005).

14. Noor, M. A. F., Grams, K. L., Bertucci, L. A. & Reiland, J. Chromosomal inversions and the reproductive isolation of species. *Proc. Natl. Acad. Sci.* **98**, 12084–12088 (2001).
15. Kirkpatrick, M. & Barton, N. Chromosome inversions, local adaptation and speciation. *Genetics* **173**, 419–434 (2006).
16. Feder, J. L., Nosil, P. & Flaxman, S. M. Assessing when chromosomal rearrangements affect the dynamics of speciation: implications from computer simulations. *Front. Genet.* **5**, 295 (2014).
17. Feder, J. L., Gejji, R., Yeaman, S. & Nosil, P. Establishment of new mutations under divergence and genome hitchhiking. *Philos. Trans. R. Soc. B Biol. Sci.* **367**, 461–474 (2012).
18. Feder, J. L. & Nosil, P. The efficacy of divergence hitchhiking in generating genomic islands during ecological speciation. *Evol. Int. J. Org. Evol.* **64**, 1729–1747 (2010).
19. Barton, N. H. What role does natural selection play in speciation? *Philos. Trans. R. Soc. B Biol. Sci.* **365**, 1825–1840 (2010).
20. Schilling, M. P. *et al.* Transitions from single- to multi-locus processes during speciation with gene flow. *Genes* **9**, (2018).
21. Feder, J. L. *et al.* Genome-wide congealing and rapid transitions across the speciation continuum during speciation with gene flow. *J. Hered.* **105**, 810–820 (2014).
22. Kopp, M. *et al.* Mechanisms of assortative mating in speciation with gene flow: connecting theory and empirical Research. *Am. Nat.* **191**, 1–20 (2017).
23. Marques, D. A. *et al.* Genomics of rapid incipient speciation in sympatric threespine stickleback. *PLOS Genet* **12**, e1005887 (2016).
24. Ma, T. *et al.* Ancient polymorphisms and divergence hitchhiking contribute to genomic islands of divergence within a poplar species complex. *Proc. Natl. Acad. Sci.* **115**, E236–E243 (2018).
25. Nosil, P., Funk, D. J. & Ortiz-Barrientos, D. Divergent selection and heterogeneous genomic divergence. *Mol. Ecol.* **18**, 375–402 (2009).
26. Nosil, P., Egan, S. P. & Funk, D. J. Heterogeneous genomic differentiation between walking-stick ecotypes: ‘isolation by adaptation’ and multiple roles for divergent selection. *Evol. Int. J. Org. Evol.* **62**, 316–336 (2008).
27. Pashley, D. P. Host-associated genetic differentiation in fall armyworm (Lepidoptera: Noctuidae): a sibling species complex? *Ann. Entomol. Soc. Am.* **79**, 898–904 (1986).

28. Kergoat, G. J. *et al.* Disentangling dispersal, vicariance and adaptive radiation patterns: a case study using armyworms in the pest genus Spodoptera (Lepidoptera: Noctuidae). *Mol. Phylogenet. Evol.* **65**, 855–870 (2012).
29. Prowell, D. P., McMichael, M. & Silvain, J.-F. Multilocus genetic analysis of host use, introgression, and speciation in host strains of fall armyworm (Lepidoptera: Noctuidae). *Ann. Entomol. Soc. Am.* **97**, 1034–1044 (2004).
30. Gouin, A. *et al.* Two genomes of highly polyphagous lepidopteran pests (Spodoptera frugiperda , Noctuidae) with different host-plant ranges. *Sci. Rep.* **7**, 11816 (2017).
31. Hänniger, S. *et al.* Genetic basis of allochronic differentiation in the fall armyworm. *BMC Evol. Biol.* **17**, 68 (2017).
32. Schöfl, G., Heckel, D. G. & Groot, A. T. Time-shifted reproductive behaviours among fall armyworm (Noctuidae: Spodoptera frugiperda) host strains: evidence for differing modes of inheritance. *J. Evol. Biol.* **22**, 1447–1459 (2009).
33. Unbehend, M., Hänniger, S., Meagher, R. L., Heckel, D. G. & Groot, A. T. Pheromonal divergence between two strains of Spodoptera frugiperda. *J. Chem. Ecol.* **39**, 364–376 (2013).
34. Dumas, P. *et al.* Spodoptera frugiperda (Lepidoptera: Noctuidae) host-plant variants: two host strains or two distinct species? *Genetica* **143**, 305–316 (2015).
35. Ruan, J. *smartdenovo: Ultra-fast de novo assembler using long noisy reads*. (2017).
36. Simão, F. A., Waterhouse, R. M., Ioannidis, P., Kriventseva, E. V. & Zdobnov, E. M. BUSCO: assessing genome assembly and annotation completeness with single-copy orthologs. *Bioinformatics* **31**, 3210–3212 (2015).
37. Langmead, B. & Salzberg, S. L. Fast gapped-read alignment with Bowtie 2. *Nat. Methods* **9**, 357–359 (2012).
38. Li, H. *et al.* The sequence alignment/map format and SAMtools. *Bioinformatics* **25**, 2078–2079 (2009).
39. Fan, H., Ives, A. R., Surget-Groba, Y. & Cannon, C. H. An assembly and alignment-free method of phylogeny reconstruction from next-generation sequencing data. *BMC Genomics* **16**, (2015).
40. Cheng, T. *et al.* Genomic adaptation to polyphagy and insecticides in a major East Asian noctuid pest. *Nat. Ecol. Evol.* **1**, 1747–1756 (2017).

41. Huelsenbeck, J. P. & Hillis, D. M. Success of phylogenetic methods in the four-taxon case. *Syst. Biol.* **42**, 247–264 (1993).
42. Frichot, E., Mathieu, F., Trouillon, T., Bouchard, G. & François, O. Fast and efficient estimation of individual ancestry coefficients. *Genetics* **196**, 973–983 (2014).
43. Nagoshi, R. N. The fall armyworm Triosephosphate Isomerase (Tpi) gene as a marker of strain identity and interstrain mating. *Ann. Entomol. Soc. Am.* **103**, 283–292 (2010).
44. Chen, K. *et al.* BreakDancer: an algorithm for high-resolution mapping of genomic structural variation. *Nat. Methods* **6**, 677–681 (2009).
45. Fariello, M. I., Boitard, S., Naya, H., SanCristobal, M. & Servin, B. Detecting signatures of selection through haplotype differentiation among hierarchically structured populations. *Genetics* **193**, 929–941 (2013).
46. Cruickshank, T. E. & Hahn, M. W. Reanalysis suggests that genomic islands of speciation are due to reduced diversity, not reduced gene flow. *Mol. Ecol.* **23**, 3133–3157 (2014).
47. Wei, Y. & Lilly, M. A. The TORC1 inhibitors Nprl2 and Nprl3 mediate an adaptive response to amino-acid starvation in Drosophila. *Cell Death Differ.* **21**, 1460–1468 (2014).
48. Jacinto, E. & Hall, M. N. TOR signalling in bugs, brain and brawn. *Nat. Rev. Mol. Cell Biol.* **4**, 117–126 (2003).
49. Lefort, V., Desper, R. & Gascuel, O. FastME 2.0: a comprehensive, accurate, and fast distance-based phylogeny inference program. *Mol. Biol. Evol.* **32**, 2798–2800 (2015).
50. Dumas, P. *et al.* Phylogenetic molecular species delimitations unravel potential new species in the pest genus Spodoptera Guenée, 1852 (Lepidoptera, Noctuidae). *PLOS ONE* **10**, e0122407 (2015).
51. Haller, B. C. & Messer, P. W. SLiM 2: flexible, interactive forward genetic simulations. *Mol. Biol. Evol.* **34**, 230–240 (2017).
52. Charlesworth, B. The effects of deleterious mutations on evolution at linked sites. *Genetics* **190**, 5–22 (2012).
53. Song, S. V., Downes, S., Parker, T., Oakeshott, J. G. & Robin, C. High nucleotide diversity and limited linkage disequilibrium in Helicoverpa armigera facilitates the detection of a selective sweep. *Heredity* **115**, 460–470 (2015).

54. Sved, J. A., Cameron, E. C. & Gilchrist, A. S. Estimating effective population size from linkage disequilibrium between unlinked loci: theory and application to fruit fly outbreak populations. *PLOS ONE* **8**, e69078 (2013).
55. Rutila, J. E. *et al.* Cycle is a second bHLH-PAS clock protein essential for circadian rhythmicity and transcription of Drosophila period and timeless. *Cell* **93**, 805–814 (1998).
56. Anderson, C. J. *et al.* Hybridization and gene flow in the mega-pest lineage of moth, Helicoverpa. *Proc. Natl. Acad. Sci.* **115**, 5034–5039 (2018).
57. Martin, S. H. *et al.* Natural selection and genetic diversity in the butterfly Heliconius melpomene. *Genetics* **203**, 525–541 (2016).
58. Li, H. & Durbin, R. Inference of human population history from individual whole-genome sequences. *Nature* **475**, 493–496 (2011).
59. Keightley, P. D. *et al.* Estimation of the spontaneous mutation rate in Heliconius melpomene. *Mol. Biol. Evol.* **32**, 239–243 (2015).
60. Riesch, R. *et al.* Transitions between phases of genomic differentiation during stick-insect speciation. *Nat. Ecol. Evol.* **1**, 82 (2017).
61. Martin, S. H. *et al.* Genome-wide evidence for speciation with gene flow in Heliconius butterflies. *Genome Res.* **23**, 1817–1828 (2013).
62. Pashley, D. P. Host-associated differentiation in armyworms (Lepidoptera: Noctuidae): An allozymic and mtDNA perspective. *Electrophor. Stud. Agric. Pests* (1989).
63. Lu, Y. J., Kochert, G. D., Isenhour, D. J. & Adang, M. J. Molecular characterization of a strain-specific repeated DNA sequence in the fall armyworm Spodoptera frugiperda (Lepidoptera: Noctuidae). *Insect Mol. Biol.* **3**, 123–130 (1994).
64. Kajitani, R. *et al.* Efficient de novo assembly of highly heterozygous genomes from whole-genome shotgun short reads. *Genome Res.* **24**, 1384–1395 (2014).
65. Gurtowski, J. *ectools: tools for error correction and working with long read data*. (2017).
66. Walker, B. J. *et al.* Pilon: an integrated tool for comprehensive microbial variant detection and genome assembly improvement. *PLOS ONE* **9**, e112963 (2014).
67. Li, H. & Durbin, R. Fast and accurate long-read alignment with Burrows–Wheeler transform. *Bioinformatics* **26**, 589–595 (2010).

68. Sahlin, K., Chikhi, R. & Arvestad, L. Assembly scaffolding with PE-contaminated mate-pair libraries. *Bioinformatics* **32**, 1925–1932 (2016).
69. Rizk, G., Gouin, A., Chikhi, R. & Lemaitre, C. MindTheGap : integrated detection and assembly of short and long insertions. *Bioinformatics* btu545 (2014). doi:10.1093/bioinformatics/btu545
70. Cantarel, B. L. *et al.* MAKER: An easy-to-use annotation pipeline designed for emerging model organism genomes. *Genome Res.* **18**, 188–196 (2008).
71. RepeatMasker Home Page. Available at: http://www.repeatmasker.org/. (Accessed: 13th October 2017)
72. Legeai, F. *et al.* Establishment and analysis of a reference transcriptome for Spodoptera frugiperda. *BMC Genomics* **15**, 704 (2014).
73. Grabherr, M. G. *et al.* Full-length transcriptome assembly from RNA-Seq data without a reference genome. *Nat. Biotechnol.* **29**, 644–652 (2011).
74. Korf, I. Gene finding in novel genomes. *BMC Bioinformatics* **5**, 59 (2004).
75. Stanke, M., Schöffmann, O., Morgenstern, B. & Waack, S. Gene prediction in eukaryotes with a generalized hidden Markov model that uses hints from external sources. *BMC Bioinformatics* **7**, 62 (2006).
76. Schubert, M., Lindgreen, S. & Orlando, L. AdapterRemoval v2: rapid adapter trimming, identification, and read merging. *BMC Res. Notes* **9**, 88 (2016).
77. *picard: A set of command line tools (in Java) for manipulating high-throughput sequencing (HTS) data and formats such as SAM/BAM/CRAM and VCF*. (Broad Institute, 2018).
78. Danecek, P. *et al.* The variant call format and VCFtools. *Bioinformatics* **27**, 2156–2158 (2011).
79. Abraham, G., Qiu, Y. & Inouye, M. FlashPCA2: principal component analysis of Biobank-scale genotype datasets. *Bioinformatics* **33**, 2776–2778 (2017).
80. Stephens, Z. D. *et al.* Simulating next-generation sequencing datasets from empirical mutation and sequencing models. *PLOS ONE* **11**, e0167047 (2016).
81. Löytynoja, A. Phylogeny-aware alignment with PRANK. *Methods Mol. Biol.* **1079**, 155–170 (2014).

Table 1. Summary statistics of genome assemblies produced in this study (New assembly) and published assembly[30] from corn and rice strains.

	Corn strain		Rice strain	
statistics	New assembly	Gouin et al	New assembly	Gouin et al
Assembly size	384,358,373	437,873,304	379,902,278	371,020,040
number of sequences	1,000	41,577	1,054	29,127
Longest sequence (bp)	5,279,935	943,242	7,849,854	314,108
Shortest sequence (bp)	8,866	888	10,636	500
N50	900,335	52,781	1,129,192	28,526
L50	124	1,616	91	3,761
N90	196,225	3,545	165,330	6,422
L90	450	18,789	421	13,881
%GC	36.3432	35.0770	36.3724	36.0741
%N	0.0689	2.5989	0.0006	0.0352

Table 2. The number of genes within genomic islands of differentiation that are potentially associated with interactions with host-plants.

Functions	refC	refR
Chemosensory	3	3
Immunity	1	0
Oxidative stress	10	9
Development	4	4
P450	1	3
Circadian Signaling	0	1
Esterase	0	2
Serine Protease	0	1

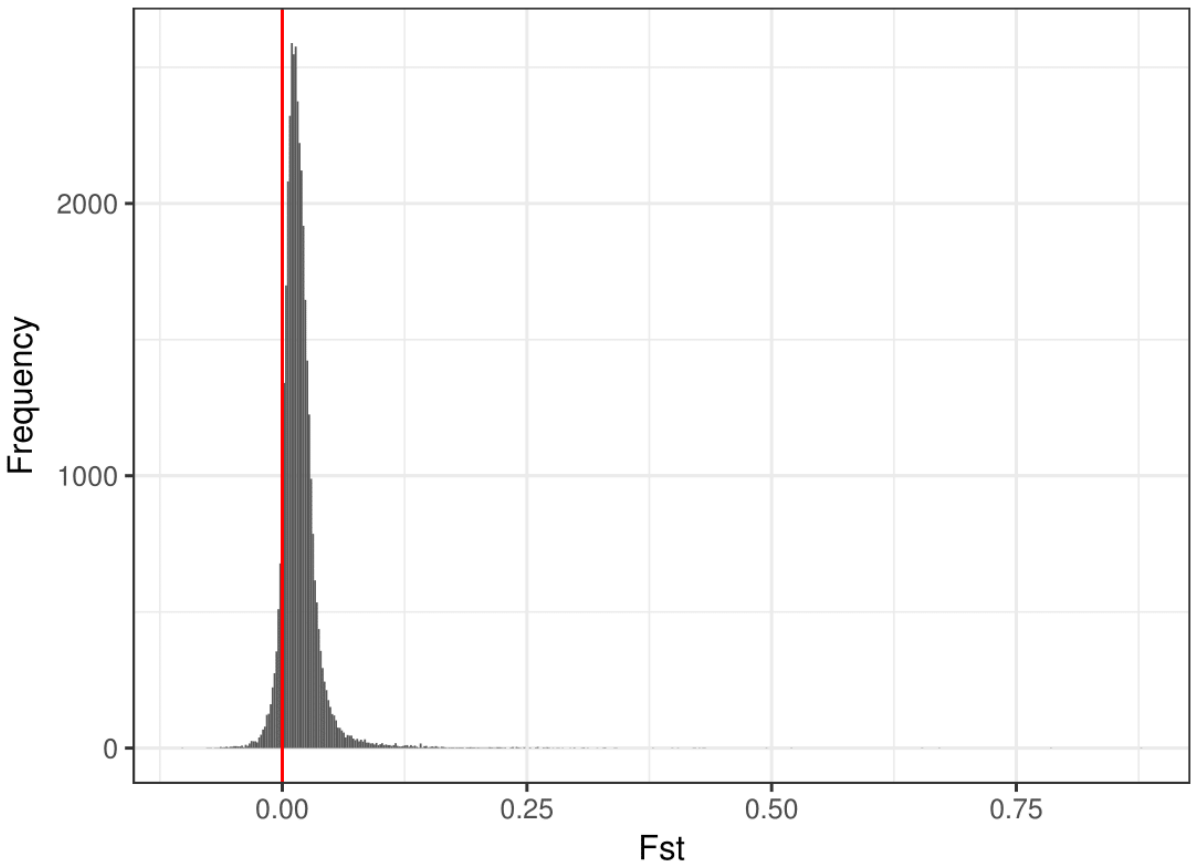

Figure 1. **The distribution of Fst calculated in 10 kb window** The red vertical line indicates Fst = 0, which means no genetic differentiation between corn and rice strains.

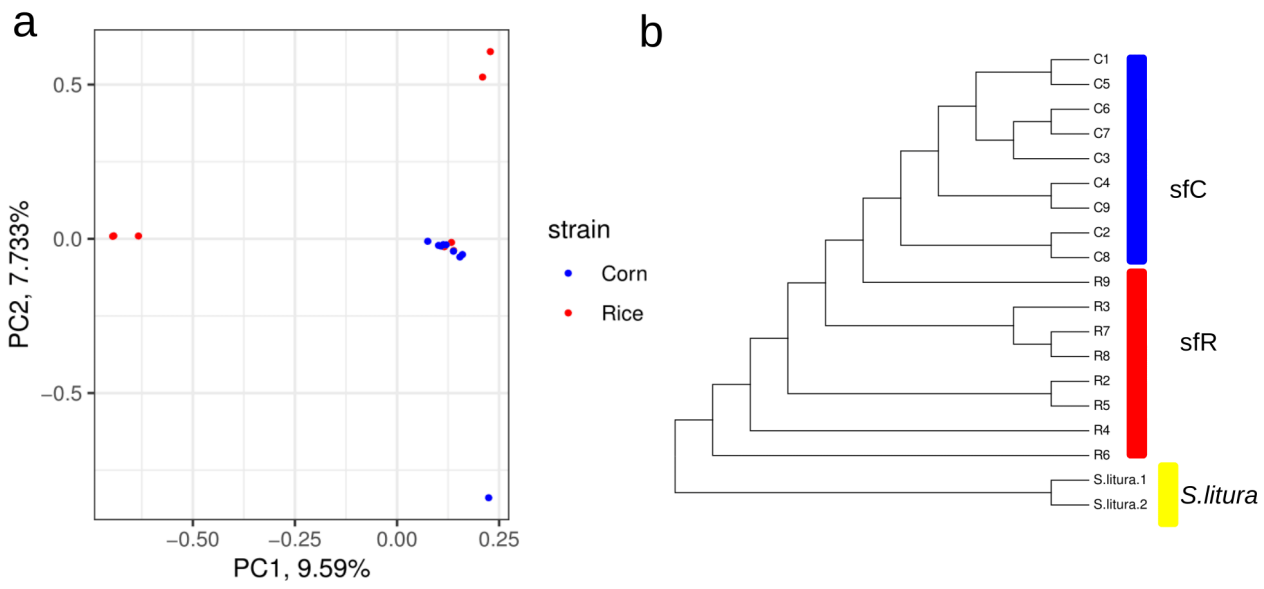

Figure 2. **Genetic relationship between corn and rice strains** a) The result from principal component analysis. The red and blue circles represent individuals from corn and rice strains, respectively. b) Phylogenetic tree reconstructed using AAF approach.

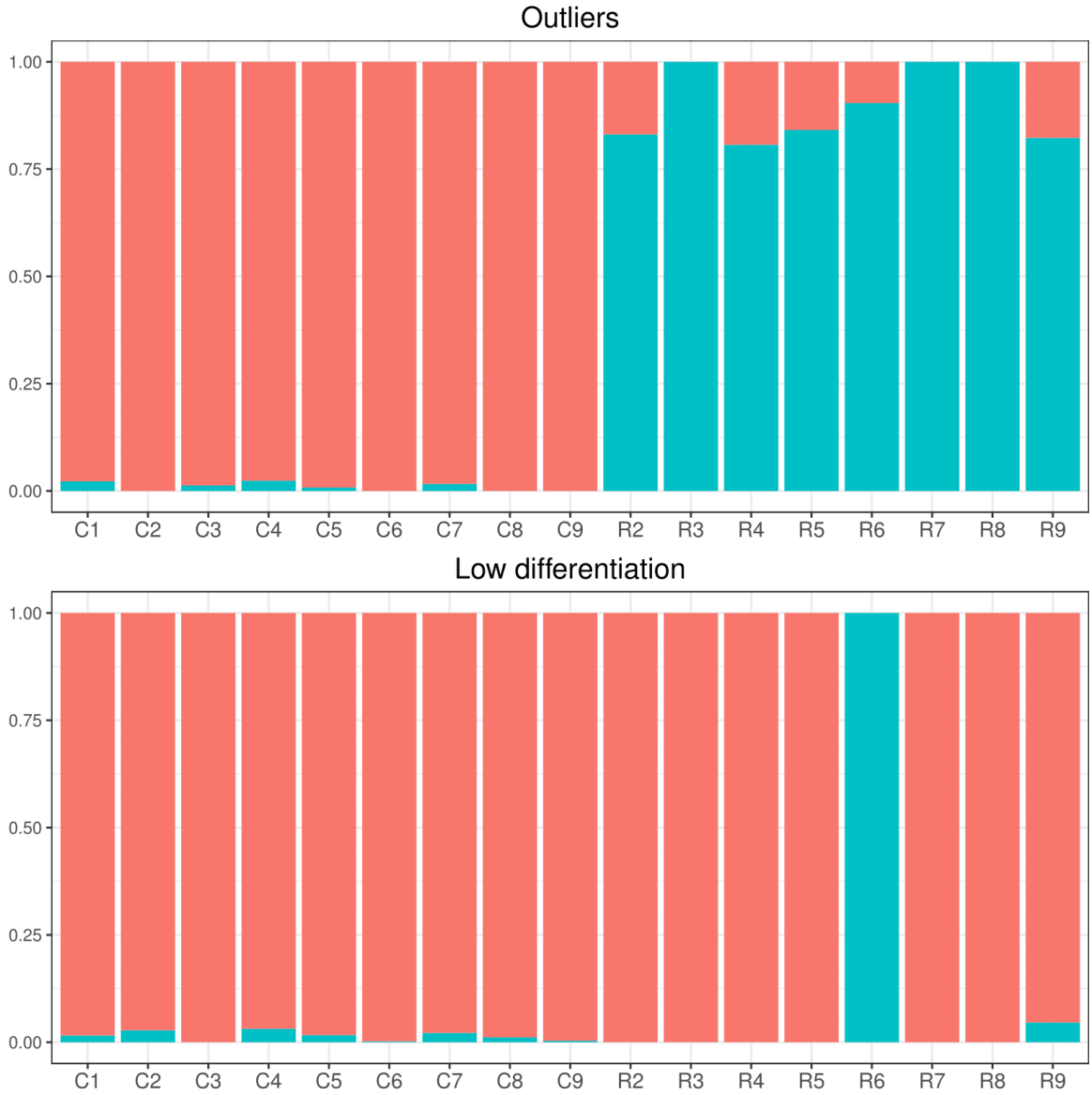

Figure 3. **Testing the divergence hitchhiking model**. Ancestry coefficient calculated from the outliers of genetic differentiation (upper) and lowly differentiated sequences (hapflk score < 1, 154,163bp in size) (bottom).

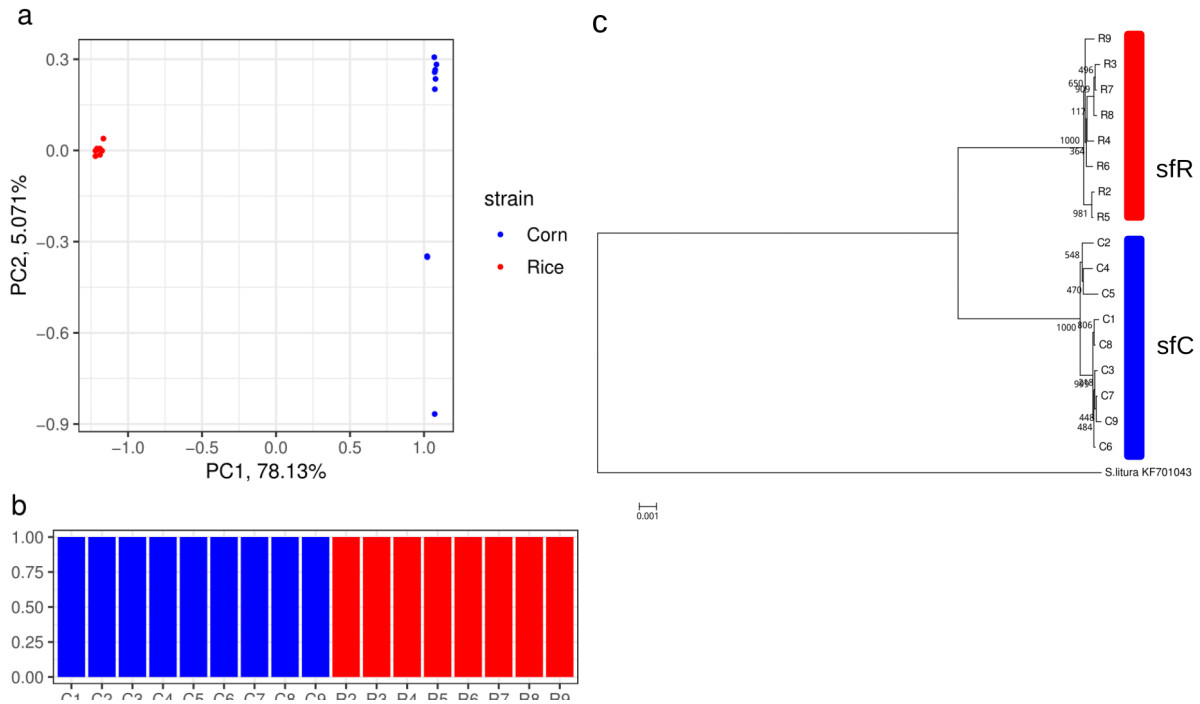

Figure 4. **Genetic relationship between corn and rice strains in the mitochondrial genome**. a) The result from principal component analysis. The red and blue circles represent individuals from sfC ad sfR, respectively. b) Ancestry coefficient results at K = 2. c) Phylogenetic tree reconstructed using minimum evolution approach.

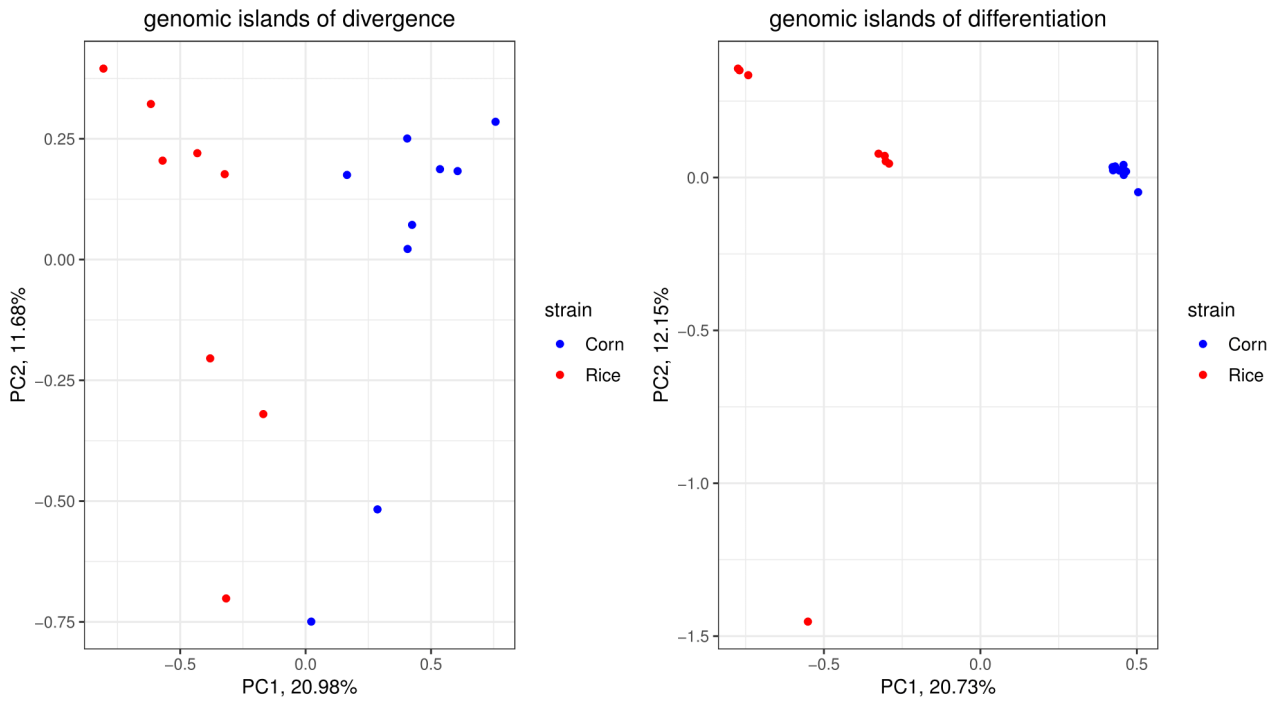

Figure 5. **Genetic relationship among individuals in outliers of genetic differentiation** The result of principal component analysis from genomic islands of divergence (left), which have higher level of both relative level of genetic differentiation (hapflk score) and absolute level of genetic divergence (d_{XY}), and genomic islands of differentiation (left), which have higher level of genetic differentiation (hapflk score) only.

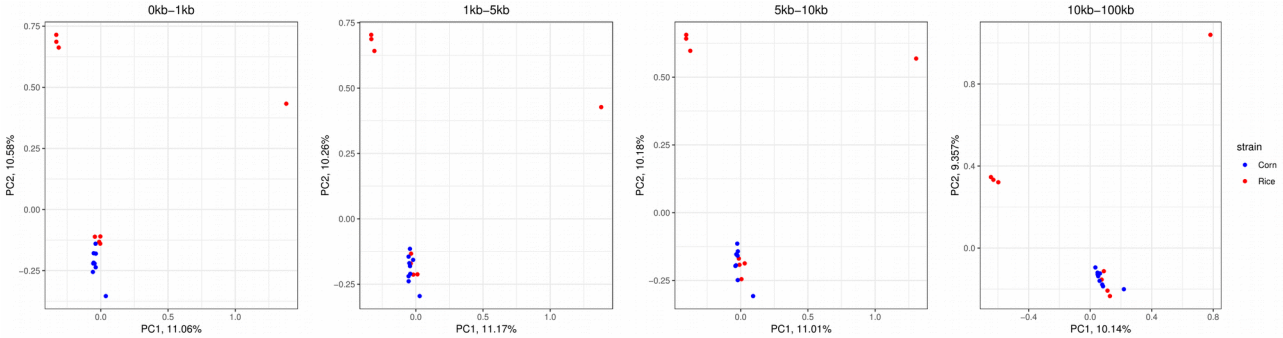

Figure 6. **The effect of physical linkage to the genomic islands of genetic differentiation** The result of principal component analysis at varying distances from the nearest the genomic islands of genetic differentiation. The result is based on the mappings against refC. See Supplementary Figure 20 for the result based on the mapping against refR.

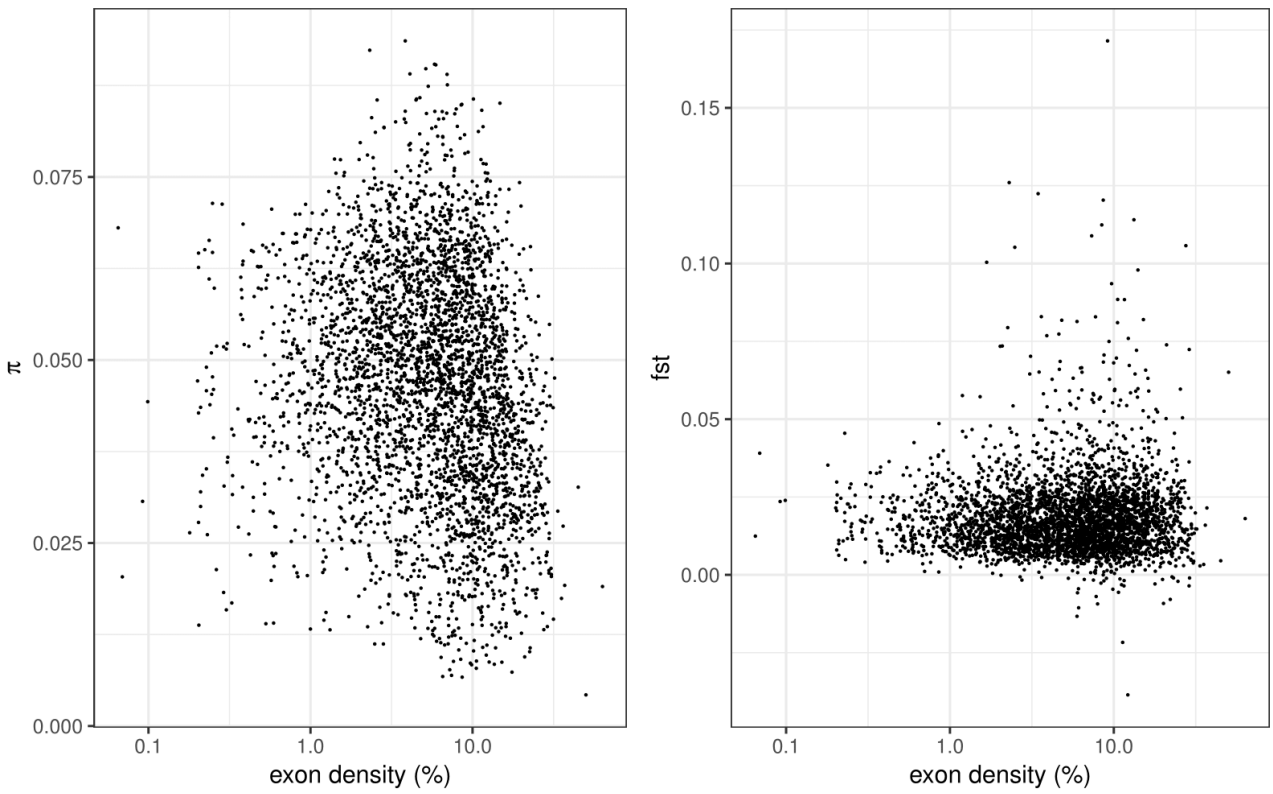

Figure 7. **The effect of selection on local variation of diversity and differentiation** Plots showing the correlation of exon density with π (left) and Fst (right) calculated from 100kb windows, based on the mapping against refC. See Supplementary Figure 21 for the result based on the mapping against refR.

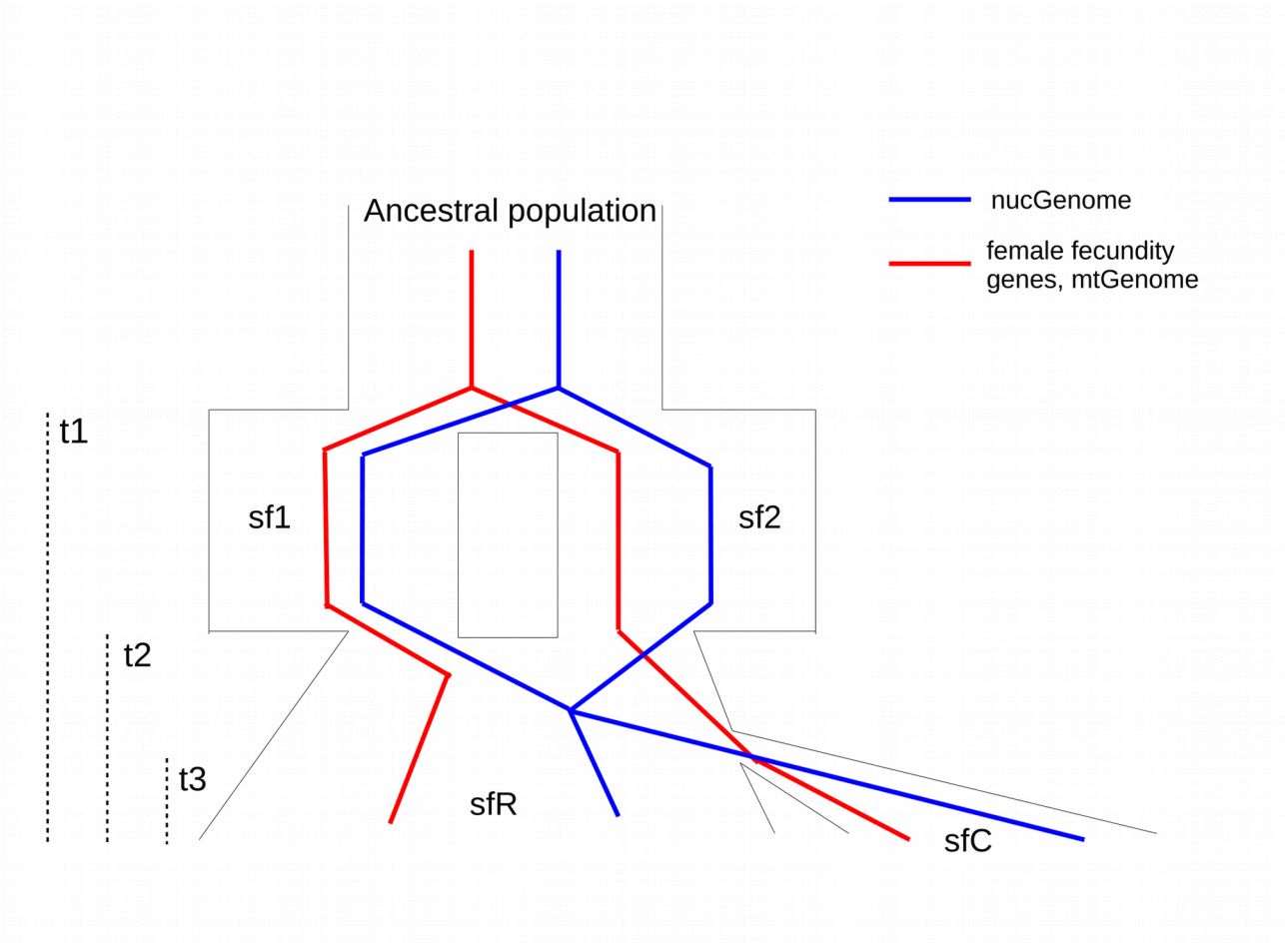

Figure 8. **A possible evolutionary scenario of genetic differentiation** The average genealogy of mitochondrial genomes and female fecundity genes (red lines) as well as nuclear genomes (blue lines) are depicted. In this scenario, an ancestral population was split into two populations, sf1 and sf2, at t1. At t2, two populations were merged by hybridization and extant sfR was generated. However, local gene flow between sf1 and sf2 was inhibited at female fecundity genes because hybrids of these genes had a reduction in fitness. Thus, the genealogy of the female fecundity genes remained separated and sequences were kept diverging. The genealogy of mitochondiral genomes is the same with the female fecundity genes because of selection on females and maternal inheritance. After t3, divergent selection targeting many genes caused a genetic differentiation according to the sequences of mitochondrial genomes and female fecundity genes by reducing genomic migration rate, and extant sfC was generated.